

*Acta Cryst.* (1999). **A55**, 457–465

## Three-wave grazing-incidence X-ray diffraction from thin crystal surface layers: determination of triplet phase invariants

YURI P. STETSKO<sup>a</sup> AND SHIH-LIN CHANG<sup>b,c,\*</sup>

<sup>a</sup>*Chernovtsy State University, Chernovtsy 274012, Ukraine,* <sup>b</sup>*Department of Physics, National Tsing Hua University, Hsinchu 30043, Taiwan,* and <sup>c</sup>*Synchrotron Radiation Research Center, Hsinchu 30077, Taiwan.*  
E-mail: [slchang@phys.nthu.edu.tw](mailto:slchang@phys.nthu.edu.tw)

(Received 15 September 1997; accepted 23 September 1998)

### Abstract

Numerical calculation of the angular and spectral distributions of the intensities of the specularly diffracted waves in the case of three-wave grazing-incidence X-ray diffraction is carried out using the dynamical theory. The angular and spectral distributions are shown to be uniquely and continuously dependent upon the value of the triplet phase invariant. A method of determining the value of the triplet phase invariant for thin crystal surface layers is developed, based on the comparison of experimentally measured three-wave peak profiles with the profiles calculated for different values of the triplet phase invariant. An analysis scheme of the phase sensitivity of the reflection coefficients is proposed taking into account the interference of the directly excited and the ‘*Umweg*’-excited specularly diffracted waves.

### 1. Introduction

Two-wave X-ray diffraction intensity measurement usually provides no phase information on the structure-factor involved. However, multiple-wave diffraction, unlike two-wave diffraction, is sensitive to the structure-factor interrelation between X-ray reflections. Several investigators (Kambe & Miyake, 1954; Hart & Lang, 1961; Colella, 1974; Post, 1977; Chapman *et al.*, 1981; Høier & Aanestad, 1981; Chang, 1982; Juretschke, 1982*a,b*; Chang & Valladares, 1985; Hümmner & Billy, 1986; Juretschke, 1986; Kshevetskiy *et al.*, 1987; Sheludko, 1987; Shen & Colella, 1988; Mo *et al.*, 1988; Chang & Tang, 1988; Hümmner *et al.*, 1989; Stetsko, 1990; Weckert & Hümmner, 1997; Shen, 1998) have examined the effect of X-ray reflection phases on the behaviour of multiple-wave diffraction and suggested techniques for direct experimental determination of the triplet phase invariant. The above studies deal with conventional diffraction cases associated with rather large X-ray penetration depths,  $t$ , around 1–10  $\mu\text{m}$ . Therefore, the above techniques are only applicable to the bulk of a crystal. Recent interest in the growth and analysis of

crystals that are nonuniform along the normal to a crystal surface calls for development of similar phasing techniques for thin surface layers.

The smallest X-ray penetration depth, 100–1000 Å, is achieved for grazing-incidence diffraction when the reflecting plane is normal to the crystal surface and the angle of incidence and the angle of scattering are comparable to the angle of total external reflection. Afanas'ev & Melkonyan (1983), Cowan (1985), Andreev (1985), and Hung & Chang (1993) have examined such diffraction for two-wave cases, while Andreev *et al.* (1985), Hung & Chang (1989), Stepanov *et al.* (1991), Tseng & Chang (1990), Stetsko & Chang (1997) have studied three- and four-wave cases. Tseng & Chang (1990) have also investigated the phase sensitivity of three-wave grazing-incidence diffraction and demonstrated the possibility of determining the triplet phase invariant from the angular distributions of intensities of specularly diffracted waves. However, the absence of qualitative distinctions between the intensity distributions for different values of a phase invariant hampers the development of an efficient technique for determining phase invariants. Therefore, further studies of the phase sensitivity of three-wave grazing-incidence diffraction seem to be appropriate.

### 2. Theoretical considerations

For the general case of multiple-wave diffraction, it is difficult to obtain an analytical solution to the problem of finding the amplitudes of diffracted waves. Therefore, here we employ an algorithm suggested by Stetsko & Chang (1997) for numerical analysis. According to this algorithm, a Cartesian coordinate system in reciprocal space with one of the axes  $O_z$  in the direction normal to the crystal surface is introduced in order to represent the system of  $N$  vector equations of the dynamical X-ray diffraction in a scalar form. It was shown that the system of vector equations for reflecting planes normal to the crystal surface can be solved as a system of matrix equations

$$(\mathbf{U} + z^2 \mathbf{I}_2) \mathbf{E}_2 = 0$$

$$\mathbf{E}_z = z^{-1} (\mathbf{G}^{-2} \mathbf{A} \mathbf{G}^2 \mathbf{E}_x + \mathbf{G}^{-2} \mathbf{B} \mathbf{G}^2 \mathbf{E}_y), \quad (1)$$

where

$$\mathbf{U} = \begin{pmatrix} \mathbf{A} \mathbf{G}^{-2} \mathbf{A} \mathbf{G}^2 + \mathbf{B}^2 - \mathbf{G}^2 & -\mathbf{A} \mathbf{B} + \mathbf{A} \mathbf{G}^{-2} \mathbf{B} \mathbf{G}^2 \\ -\mathbf{A} \mathbf{B} + \mathbf{B} \mathbf{G}^{-2} \mathbf{A} \mathbf{G}^2 & \mathbf{A}^2 + \mathbf{B} \mathbf{G}^{-2} \mathbf{B} \mathbf{G}^2 - \mathbf{G}^2 \end{pmatrix}. \quad (2)$$

Here, the term  $z^2$  is the eigenvalue.  $\mathbf{A}$  and  $\mathbf{B}$  are the  $N \times N$  diagonal matrices whose diagonal elements are given by  $a_{mm} = X_m - x_n$ ,  $b_{mm} = Y_m - y_n$ , where  $X_m$ ,  $Y_m$  and  $Z_m$  are the coordinates of the reciprocal-lattice sites, and  $x_n$ ,  $y_n$ ,  $z$  are the coordinates of the origins of the wave vectors in the above coordinate system. The values of  $Z_m$  are assumed to be equal (in particular,  $Z_m = 0$ ,  $m = 0, 1, \dots, N-1$ ). The matrix  $\mathbf{G}$  is defined as  $\mathbf{G}^2 = K^2(\mathbf{I} + \mathbf{F})$ , where  $K$  is the magnitude of the incident wavevector in vacuum, i.e.  $K = 1/\lambda$ ,  $\mathbf{I}$  is the  $N \times N$  unit matrix, and  $\mathbf{F}$  is the  $N \times N$  matrix whose elements are given by  $f_{mn} = \chi_{H_m} - \chi_{H_n}$ , where  $\chi_H = -r_e \lambda^2 F_H / (\pi V)$  are the Fourier components of the crystal polarizability,  $r_e$  is the classical electron radius,  $\lambda$  is the incident X-ray wavelength,  $F_H$  is the structure factor and  $V$  is the unit-cell volume. The eigenvectors  $\mathbf{E}_x = (E_0^x, E_1^x, \dots, E_{N-1}^x)^T$ ,  $\mathbf{E}_y = (E_0^y, E_1^y, \dots, E_{N-1}^y)^T$ ,  $\mathbf{E}_z = (E_0^z, E_1^z, \dots, E_{N-1}^z)^T$  are the vector columns of unknown components of electrical vectors  $\mathbf{E}_{H_m} = E_m^x \mathbf{i} + E_m^y \mathbf{j} + E_m^z \mathbf{k}$ .  $\mathbf{I}_2$  is the  $2N \times 2N$  unit matrix and the column  $\mathbf{E}_2 = [(\mathbf{E}_x)^T, (\mathbf{E}_y)^T]^T$ .

The solution of equation (1) is reduced to finding the eigenvalues  $-z^2$  and eigenvectors of the scattering matrix  $\mathbf{U}$ . For convenience,  $\mathbf{G}^{-2} = K^{-2}(\mathbf{I} + \mathbf{F})^{-1}$  can be taken as  $\mathbf{G}^{-2} = K^{-2}(\mathbf{I} - \mathbf{F})$  to within the order of magnitude of  $\chi^2$ . The matrix  $\mathbf{U}$  then takes the form

$$\mathbf{U} = \begin{pmatrix} \mathbf{A}^2 + \mathbf{B}^2 - \mathbf{G}^2 + \mathbf{A} \mathbf{F} \mathbf{A} & \mathbf{A} \mathbf{F} \mathbf{B} \\ \mathbf{B} \mathbf{F} \mathbf{A} & \mathbf{A}^2 + \mathbf{B}^2 - \mathbf{G}^2 + \mathbf{B} \mathbf{F} \mathbf{B} \end{pmatrix}, \quad (3)$$

where  $\mathbf{F}_A = \mathbf{A} \mathbf{F} - \mathbf{F} \mathbf{A}$ ,  $\mathbf{F}_B = \mathbf{B} \mathbf{F} - \mathbf{F} \mathbf{B}$ .

Leaving out lengthy trivial transformations, the dispersion equation  $\det(\mathbf{U} + z^2 \mathbf{I}_2) = 0$  in the vicinity of the Lorentz multiple-wave point for the three-wave case under discussion becomes

$$c_0 c_1 c_2 - K^4 (c_0 r_{12} + c_1 r_{20} + c_2 r_{01}) + K^6 q = 0 \quad (4a)$$

$$c_0 c_1 c_2 - (c_0 p_{12}^2 r_{12} + c_1 p_{20}^2 r_{20} + c_2 p_{01}^2 r_{01}) + p_{12} p_{20} p_{01} q = 0 \quad (4b)$$

where

$$c_m = z^2 + a_{mm}^2 + b_{mm}^2 - K^2(1 + \chi_0)$$

$$r_{mn} = \chi_{H_m - H_n} \chi_{H_n - H_m}$$

$$q = \chi_{-H_1} \chi_{H_2} \chi_{H_1 - H_2} + \chi_{H_1} \chi_{-H_2} \chi_{H_2 - H_1}$$

$$p_{mn} = a_{mn} a_{nn} + b_{mn} b_{nn}, \quad m, n = 0, 1, 2.$$

It can be easily seen that the dispersion equation (4a) is similar to the dispersion equation for  $\sigma$  polarization mentioned in the work by Tseng & Chang (1990).

### 3. The phase of the structure factor and the triplet phase invariant

Consider a three-wave  $(0, H, K)$  diffraction, where  $H$  is the primary,  $K$  is the secondary and  $L$  is the coupling reflection with the diffraction vectors  $\mathbf{H}$ ,  $\mathbf{K}$  and  $\mathbf{L} = \mathbf{H} - \mathbf{K}$  forming a triangle in the reciprocal-lattice space. Since  $-\mathbf{H} + \mathbf{K} + \mathbf{L} = 0$ , the phase  $\Phi_3$  of the structure-factor triplet  $F_{-H} F_K F_L$ ,

$$\Phi_3 = \Phi_{-H} + \Phi_K + \Phi_L, \quad (5)$$

is independent of the choice of the origin of the crystal unit cell, i.e.  $\Phi_3$  is a triplet phase invariant. Similarly, the phase  $\Phi_3^*$  of  $F_H F_{-K} F_{-L}$ ,

$$\Phi_3^* = \Phi_H + \Phi_{-K} + \Phi_{-L}, \quad (6)$$

is also a triplet phase invariant. For a non-absorbing crystal,  $\Phi_3^* = -\Phi_3$ , whereas for an absorbing crystal this equality is only accurate to within several degrees of arc.

To handle the multiple-wave diffraction for an absorbing crystal, we introduce for convenience the notion of a modified phase as follows. In view of the fact that there exists a coordinate system in which  $F_H \simeq F_{-H} \equiv \bar{F}_H$  (we neglect the differences associated with anomalous scattering), the structure factor under an arbitrary coordinate system can be represented as  $F_H = \bar{F}_H \exp(i\bar{\Phi}_H)$ , where  $\bar{\Phi}_H$  is a modified phase. For a non-absorbing crystal,  $\bar{\Phi}_H = \Phi_H$ , and  $\bar{F}_H$  is a real value. For an absorbing crystal,  $\bar{\Phi}_H$  differs from  $\Phi_H$  by several degrees of arc and  $\bar{F}_H$  is a complex quantity whose imaginary part is responsible for X-ray absorption. Under such a definition of a phase,  $\bar{\Phi}_{-H} = -\bar{\Phi}_H$ , while, for modified triplet phase invariants  $\bar{\Phi}_3 = \bar{\Phi}_{-H} + \bar{\Phi}_K + \bar{\Phi}_L$  and  $\bar{\Phi}_3^* = \bar{\Phi}_H + \bar{\Phi}_{-K} + \bar{\Phi}_{-L}$ , the condition  $\bar{\Phi}_3^* = -\bar{\Phi}_3$  is fulfilled, regardless of the absorption. For consistency, in what follows we use the triplet phase invariant  $\bar{\Phi}_3$ .

Since it is a straightforward matter to determine the  $\bar{F}_H$  value from the measured intensities of two-wave reflections, one should be able to determine the triplet phase invariant  $\bar{\Phi}_3$  from the measured intensities of three-wave X-ray reflections. Note that no structure-factor modulus is assumed to be equal or close enough to zero value; otherwise, the value of the triplet phase invariant would be indeterminate.

### 4. A technique for direct determination of the triplet phase invariant

To determine the triplet phase invariant for a thin surface layer, we consider a three-wave configuration Si (000, 440, 404) using linearly  $\pi$ -polarized radiation with the electric field vector lying in the plane of reflection

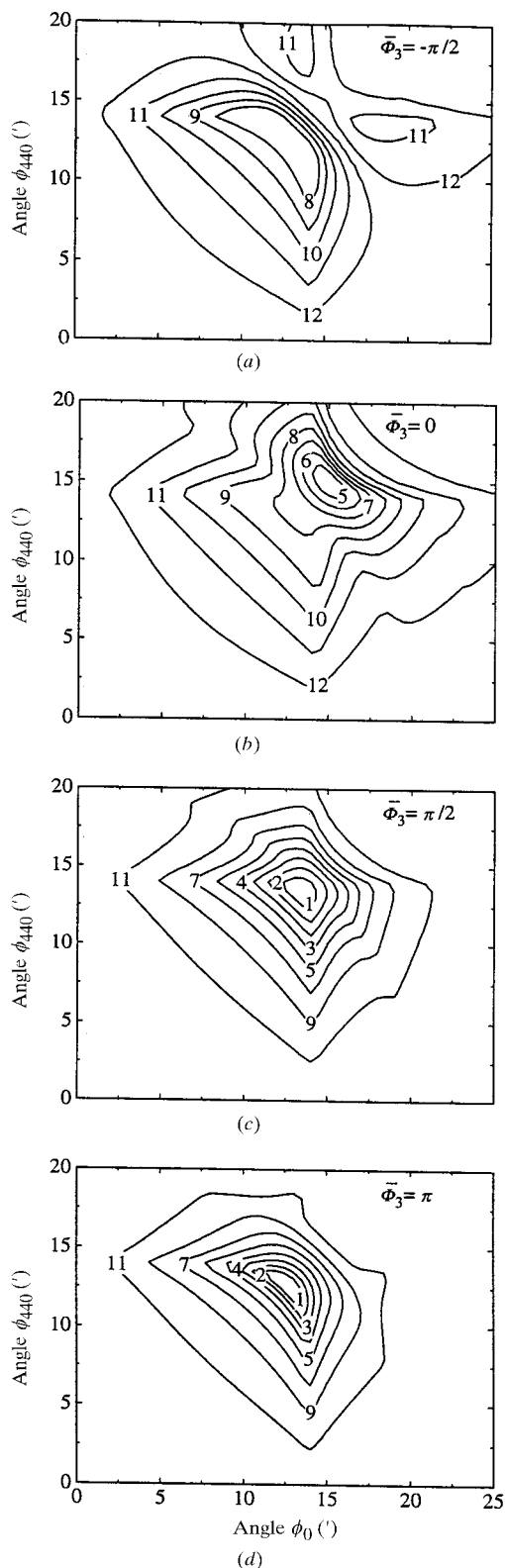


Fig. 1. Reflection coefficient  $R_{440}(\phi_0, \phi_{440})$  for the triplet phase invariants  $\bar{\Phi}_3 = -\pi/2, 0, \pi/2, \pi$ . Contours 1–12 correspond to  $R_{440} = 0.16, 0.14, 0.12, 0.1, 0.08, 0.07, 0.06, 0.05, 0.04, 0.03, 0.02, 0.01$ .

(440). As was shown by Stetsko & Chang (1997), the three-wave interaction of grazing X-ray beams is of a coincidental nature. Hence, calculations are carried out here for different incident wavelengths. The exact multiple-wave diffraction condition is that the multiple-wave Lorentz point should be in the plane of configuration. The wavelength satisfying this condition is given by  $\lambda_M = 1.66286 \text{ \AA}$ . The spectral parameter is taken to be  $S = (\lambda_M - \lambda)/\lambda_M$ . Thus, the exact multiple-wave diffraction condition will be given by  $S = 0$ . Calculations were carried out using the polarizability Fourier components  $\chi_0 = -(1.762 + i0.507) \times 10^{-5}$ ,  $\chi_{440} = \chi_{404} = \chi_{044} = -(0.694 + i0.463) \times 10^{-5}$  calculated for Si and the aforementioned wavelength.

We first consider the phase sensitivity of the angular distribution  $R_{440}(\phi_0, \phi_{440})$  of the reflection coefficient of a specularly diffracted wave for  $S = 0$ . In Fig. 1, the calculated  $R_{440}$  for various triplet phase invariants,  $\bar{\Phi}_3 = -\pi/2, 0, \pi/2, \pi$ , are shown. Here,  $\phi_0$  and  $\phi_{440}$  are the incident and exit angles. It can be seen that the variations of triplet phase invariant produce no qualitative changes in the angular distribution of the reflection coefficient of a specularly diffracted wave. Moreover, in view of the aforementioned arbitrary nature of multiple-wave diffraction, a direct measurement of the angular intensity distributions of a specularly diffracted wave requires that the wavelength of the monochromatic incident radiation satisfies the exact condition for multiple-wave diffraction or, at least, one should be able to determine with a high degree of accuracy the limiting values of deviations from this condition. The above considerations explain the difficulties arising in determining the triplet phase invariants by comparing the calculated and the measured angular distributions of the reflection coefficients.

To eliminate these difficulties, Stetsko & Chang (1997) proposed to perform spectral scanning of the multiple-wave region. One practical way of spectral scanning of the multiple-wave region is as follows. Consider a highly monochromatic beam incident on a crystal surface at a fixed angle  $\phi_0$  within the total-external-reflection region and well collimated within the incident angle. The beam is divergent over an azimuthal angle  $\phi_0$ , *i.e.* the angle of rotation of a crystal around the normal to its entrance surface. Generally, one can use an arbitrary incidence angle  $\phi_c$  within the total external reflection region. However, it seems rational to employ an incidence angle equal to the critical angle  $\phi_c = (|\chi_0|)^{1/2}$ , which enables one to unify the method for various grazing-incidence multiple-wave diffraction cases. Fig. 2 shows the calculated spectral and angular distributions  $R_{440}(S, \phi_0)$  for triplet phase invariants  $\bar{\Phi}_3 = -\pi/2, 0, \pi/2, \pi$ . The origin  $\phi_0 = 0$  is chosen so that  $\phi_{440} = 0$ . The three-wave interaction region under these coordinates is seen to exhibit two directions, one parallel to the spectral axis  $S$  and the other inclined to it at an angle, such that  $\Delta\phi_0 = \Delta S(\tan \theta_{440} + \tan \theta_{404})$ .

where  $\theta_{440}$  and  $\theta_{404}$  are the diffraction angles. A departure from the position  $S = 0$  corresponds to a transition from the three-wave into the two-wave region. Fig. 3 shows the semi-integrated reflection coefficient

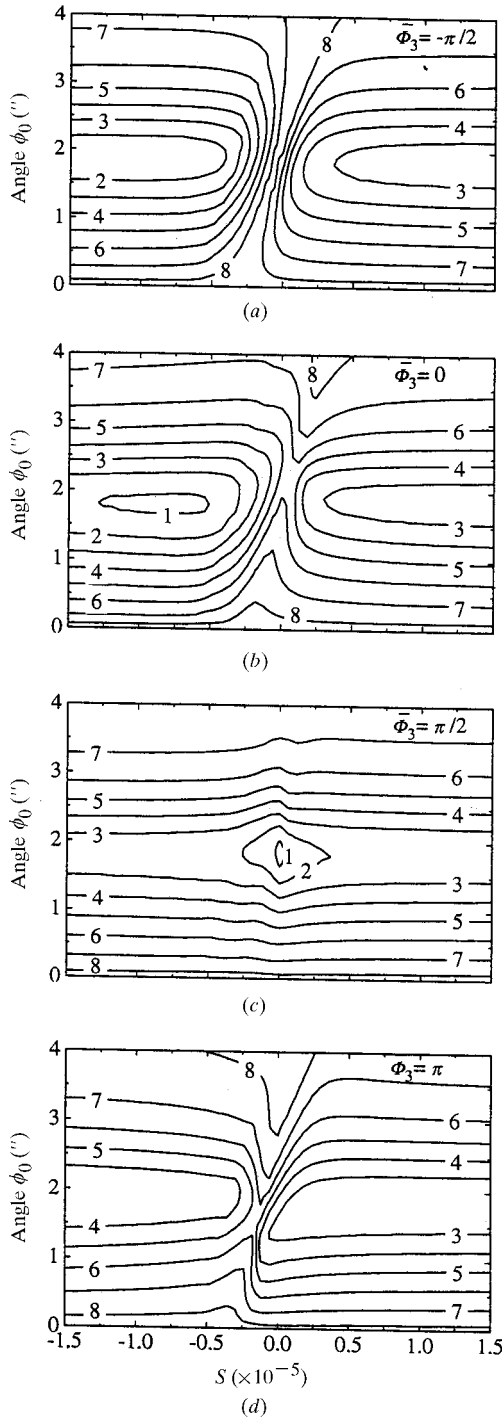


Fig. 2. Reflection coefficient  $R_{440}(S, \phi_0)$  for the triplet phase invariants  $\Phi_3 = -\pi/2, 0, \pi/2, \pi$ . Contours 1–8 correspond to  $R_{440} = 0.16, 0.14, 0.12, 0.1, 0.08, 0.06, 0.04, 0.02$ .

$R_{440}(S, \bar{\Phi}_3) = \int R_{440}(S, \bar{\Phi}_3, \phi_0) d\phi_0$  obtained under a continuously varying triplet phase invariant  $\bar{\Phi}_3$ . The  $R_{440}(S, \bar{\Phi}_3)$  values are normalized to an appropriate two-wave diffraction value. Figs. 2 and 3 exhibit close similarity between the phase dependence of three-wave peak profiles resulting from spectral scanning of an allowed specularly diffracted wave and those resulting from horizontal angular scanning of an allowed reflection using the Renninger experimental set-up (Renninger, 1937). For  $\bar{\Phi}_3 = 0$ , the local minimum and maximum appear in the reverse order compared with that for  $\bar{\Phi}_3 = \pi$ , while, for  $\bar{\Phi}_3 = -\pi/2$ , weakening [*Aufhellung* (Wagner, 1923)], and, for  $\bar{\Phi}_3 = \pi/2$ , strengthening [*Umweganregung* (Renninger, 1937)] of two-wave intensity dominates. Fig. 3 indicates that the shape of the three-wave peak of a specularly diffracted wave is a single-valued continuous function of the triplet phase invariant.

Thus, the technique for the determination of a triplet phase invariant for thin crystal surface layers is reduced to the measurement of the three-wave peak profile  $I_{\text{exp}}(S)$  and its comparison with those calculated,  $I_{\text{calc}}(S, \bar{\Phi}_3)$ , for various phase-invariant values. A proper check for correctness of the resulting triplet phase invariant could be a minimum value of the parameter

$$P(\Delta S, \bar{\Phi}_3) = \int [I_{\text{exp}}(S) - I_{\text{calc}}(S + \Delta S, \bar{\Phi}_3)]^2 dS. \quad (7)$$

The task is simplified in the case involving a thin surface layer of centrosymmetric structure. In this case, one of the two possible values of the invariant,  $\Phi_3 = 0$  or  $\pi$ , is determined in the same way from the asymmetry of a three-wave peak, *i.e.* from the order of appearance of the local minimum and maximum, as for the bulk of a crystal (Chang, 1982). Chang *et al.* (1998) recently experimentally realised the above-described technique. The experimental results are in good agreement with the theoretical results presented in this paper.

### 5. The analysis scheme of phase sensitivity

The essence of the proposed three-wave reflection model is that the intensity of a specularly diffracted wave is represented as a result of interference of the waves, of which one is due to the direct two-wave reflection, while the other is due to the *Umweganregung* of the same reflection. These two waves can be derived separately by assuming that either the secondary reflection  $K$  and the coupling reflection  $L$  or the primary reflection  $H$  are forbidden reflections.

As a first approximation, the amplitude  $E^s$  of a specularly diffracted wave  $H$  can be considered as a result of the addition of the amplitudes  $E_{\text{dir}}^s$  and  $E_{\text{um}}^s$  of a directly excited and an ‘Umweg’-excited wave:

$$E^s = E_{\text{dir}}^s + E_{\text{um}}^s \quad (8)$$

Here, the superscripts  $s$  ( $=\sigma, \pi$ ) refer to the two components of polarization with respect to the  $H$  reflection. Since under the diffraction geometry in question the wave vectors of the diffracted waves are actually coplanar, the interference of the orthogonal polarization components should be negligible; hence the amplitudes of the same polarization in expression (8) can be considered independently and separately.

### 5.1. Two-wave diffraction

We first consider the case where the  $K$  and  $L$  reflections are forbidden, *i.e.* two-wave diffraction occurs. Only the  $H$  reflection occurs. Then, using terms given by Afanas'ev & Melkonyan (1983), the amplitude of a specularly diffracted wave can be represented as

$$E_{\text{dir}}^s(\phi_0, \phi_H) = -2P_H^s \phi_0 \chi_H E_0 (u_2 - u_1) [w_2(u_1 + \phi_0) \times (u_2 + \phi_H) - w_1(u_1 + \phi_H)(u_2 + \phi_0)]^{-1}, \quad (9)$$

where  $E_0$  is the amplitude of the incident wave in vacuum and

$$w_j = -\alpha/2 \pm [\alpha^2/4 + (P_H^s)^2 \chi_H \chi_{-H}]^{1/2} \quad (10)$$

$$u_j = s_j(\phi_0^2 + w_j + \chi_0)^{1/2},$$

in which  $s_j = -\text{sign}\{\text{Im}[(\phi_0^2 + w_j + \chi_0)^{1/2}]\}$  and  $\alpha = \phi_0^2 - \phi_H^2$ .  $P_H^s$  is the polarization factor:  $P_H^\sigma = 1$  and  $P_H^\pi = \cos 2\theta_H$ , where  $\theta_H$  is the Bragg angle. Close examination of (9) indicates that the initial phase of this wave can be represented as

$$\Psi_{\text{dir}}^s = \Psi_0^s + \Delta_{\text{dir}}^s + \Phi_H, \quad (11)$$

where  $\Psi_0^s$  is the phase of the incident wave  $E_0$ ,  $\Phi_H$  the phase of the  $\chi_H$ , and  $\Delta_{\text{dir}}^s$  the phase of the rest of expression (9). Here,  $\Delta_{\text{dir}}^s$  describes the phase lag due to the diffraction and depends on the incident wavelength, incidence angles, diffraction geometry and polarization, while  $\Phi_H$  is a 'geometrical' phase shift.

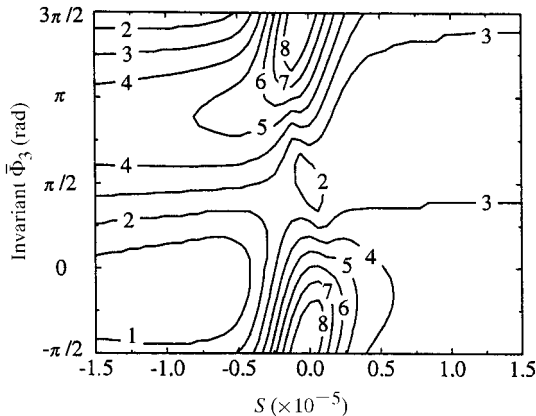


Fig. 3. Semi-integral reflection coefficient  $R_{440}(S, \bar{\Phi}_3)$ . Contours 1–8 correspond to  $R_{440} = 1.2, 1.1, 1.0, 0.9, 0.8, 0.7, 0.6, 0.5$ .

We shall now point out some of the features of the two-wave diffraction which are important for analysing the phase sensitivity. These features can be observed in Fig. 4, which shows the angular distributions of the reflection coefficient  $R_{440}(\phi_0, \phi_{440})$  and the phase  $\Delta_{\text{dir}}^\pi$  of a specularly diffracted wave for  $\pi$ -polarized radiation. The lines  $T_0$  and  $T_{440}$  represent angles  $\phi_0 = \phi_c$  and  $\phi_{440} = \phi_c$ , while the intersection of these lines gives a two-wave Lorentz point. The maximum of the reflection coefficient is observed at  $\phi_0 = \phi_{440} = (|\chi_0| - |P_{440}^\pi \chi_{440}|)^{1/2}$ . Within the two-wave region, where  $\phi_0 = \phi_{440} \rightarrow 0$ , the phase  $\Delta_{\text{dir}}^\pi$  increases from  $-\pi$  to  $\pi/2$ . Outside this region, (9) becomes

$$E_{\text{dir}}^s(\phi_0, \phi_H) = P_H^s \chi_H E_0 f(\phi_H)/\phi_0 \quad (12)$$

as  $\phi_0 \rightarrow \infty$ , where

$$f(\phi_H) = 1/[\phi_H + (\phi_H^2 + \chi_0)^{1/2}] = |f(\phi_H)| \exp[i\Delta(\phi_H)]. \quad (13)$$

The phase  $\Delta_{\text{dir}}^s$  can then be represented as

$$\Delta_{\text{dir}}^s(\phi_0, \phi_H) = \Delta(\phi_H) + \Lambda_H^s, \quad (14)$$

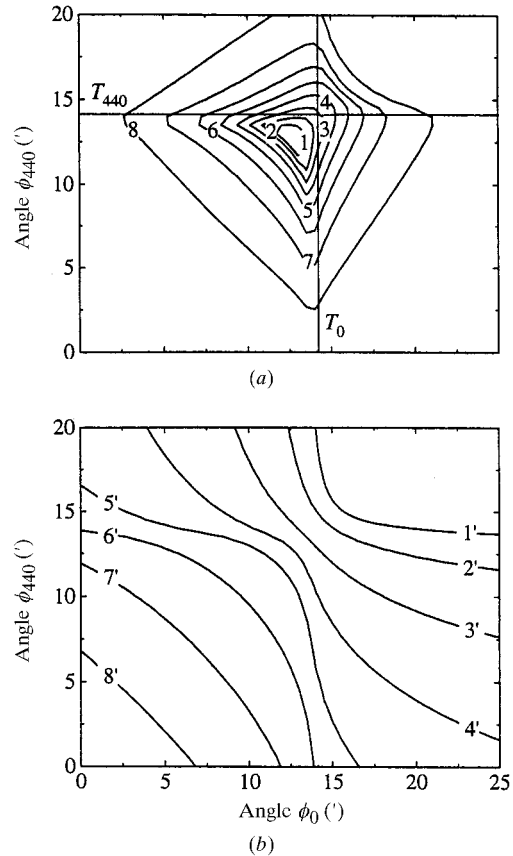


Fig. 4. Two-wave diffraction: (a) reflection coefficient  $R_{440}(\phi_0, \phi_{440})$  and (b) the phase  $\Delta_{\text{dir}}^\pi$ . Contours 1–8 (a) correspond to  $R_{440} = 0.16, 0.14, 0.12, 0.1, 0.08, 0.06, 0.04, 0.02$  and 1'–8' (b) correspond to  $\Delta_{\text{dir}}^\pi = -5\pi/6, -2\pi/3, -\pi/2, -\pi/3, -\pi/6, 0, \pi/6, \pi/3$ .

where  $\Delta(\phi_H)$  is the phase of  $f(\phi_H)$ , depending on a single angle  $\phi_H$ , while

$$\Lambda_H^s = \begin{cases} 0, & \text{if } P_H^2 > 0 \\ -\pi, & \text{if } P_H^2 < 0 \end{cases} \quad (15)$$

is defined by the polarization factor. As the angle  $\phi_H$  decreases from  $\phi_c$  to 0,  $\Delta(\phi_H)$  increases from 0 to  $\pi/2$ . The phase  $\Delta_{\text{dir}}^s$  for  $\phi_H \rightarrow \infty$  can be represented in a similar way. In a general case,  $\Delta_{\text{dir}}^s$  can be represented as

$$\Delta_{\text{dir}}^s(\phi_0, \phi_H) = \Delta(\phi_0) + \Delta(\phi_H) + \Lambda_H^s \quad (16)$$

in a first approximation. The above approximation fails only for small angles  $\phi_0, \phi_c$  in the vicinity of the Lorentz point, when the dispersion surface is at maximum distance from the spheres of radius  $(1 + \chi_0)^{1/2}/\lambda$  circumscribing the reciprocal-lattice points 0 and  $H$ .

An important point when analysing the phase sensitivity is the behaviour of the relative phase of a specularly diffracted wave when reciprocal-lattice points move out of the Ewald sphere. In particular, when lattice point  $H$  moves out of the Ewald sphere in expression (12), a transition from positive to negative  $\phi_H$  angles takes place. The latter situation corresponds to a case when the normal component of the wavevector of a specularly diffracted wave outside the crystal is an imaginary quantity and the wave outside the crystal is

exponentially damped [this is the so-called 'surface wave' or 'evanescence wave' (see Andreev *et al.*, 1982)]. It then follows from (13) that the phase  $\Delta(\phi_H)$  changes to  $\pi$  when the lattice point  $H$  moves out of the Ewald sphere.

Fig. 5 shows the distributions of the reflection coefficient and the phase  $\Delta_{\text{dir}}^s$  of a specularly diffracted wave under the coordinate system  $O_{S\phi_0}$  for the two-wave (440) case. These distributions exhibit no dependence on the spectral parameter. They are given here solely to preserve the wholeness of the exposition of the phase-sensitivity mechanism.

### 5.2. Umweganregung three-wave diffraction

Let the primary reflection  $H$  be forbidden and the  $K$  and  $L$  reflections be allowed. In the first approximation, the *Umweg*-excited wave can be viewed as a result of sequential reflections of an incident wave by the two crystal planes,  $K$  and  $L$ . Therefore, the initial phase of such a wave can be written as

$$\Psi_{\text{um}}^s = \Psi_0^s + \Delta_{\text{um}}^s + \Phi_K + \Phi_L, \quad (17)$$

where  $\Delta_{\text{um}}^s$ , just as  $\Delta_{\text{dir}}^s$  in (11), depends only on the wavelength and the angles of incidence.

The angular distributions of the reflection coefficient  $R_{440}(\phi_0, \phi_{440})$  and the phase  $\Delta_{\text{um}}^s$  of a specularly diffracted wave for  $S = 0$  are shown in Fig. 6. The arcs  $T_{404}$  and  $T'_{440}$  are associated with the angles  $\phi_{404} = \phi_c$  and  $\phi_{404} = 0$  in the coordinate system  $O_{\phi_0\phi_{440}}$ . The intersection of lines  $T_0$ ,  $T_{440}$  and  $T_{404}$  is the three-wave Lorentz point. The reflection region exhibits three intersecting bands extended along the lines  $T_0$ ,  $T_{440}$  and  $T_{404}$ , which is typical for *Umweganregung*. The maximum of the reflection coefficient is observed at the Lorentz point. The phase  $\Delta_{\text{um}}^s$  exhibits a rather complex angular distribution. However, at some distance from the Lorentz point it can be expressed in the form

$$\Delta_{\text{um}}^s(\phi_0, \phi_H) = \Delta(\phi_0) + \Delta(\phi_H) + \Delta(\phi_K) + \Lambda_K^s + \Lambda_L^s \quad (18)$$

just as (16) in §5.1. Here, the angle  $\phi_K$  depends on the angles  $\phi_0$  and  $\phi_H$ . By analogy with the two-wave diffraction,  $\Delta_{\text{um}}^s$  changes to  $\pi$  when lattice point  $K$  moves out of the Ewald sphere, *i.e.* when a transition from positive to negative  $\phi_K$  angles takes place.

Fig. 7 shows the spectral and angular distributions of the reflection coefficient and the phase  $\Delta_{\text{um}}^s$  of a specularly diffracted wave in the vicinity of the three-beam diffraction position. The reflection region in the coordinate system  $O_{S\phi_0}$  exhibits two intersecting bands extended along the lines  $T_{440}$  and  $T_{404}$ , which is typical for *Umweganregung*. Again, when the lattice point  $K$  moves out of the Ewald sphere,  $\Delta_{\text{um}}^s$  changes to  $\pi$ .

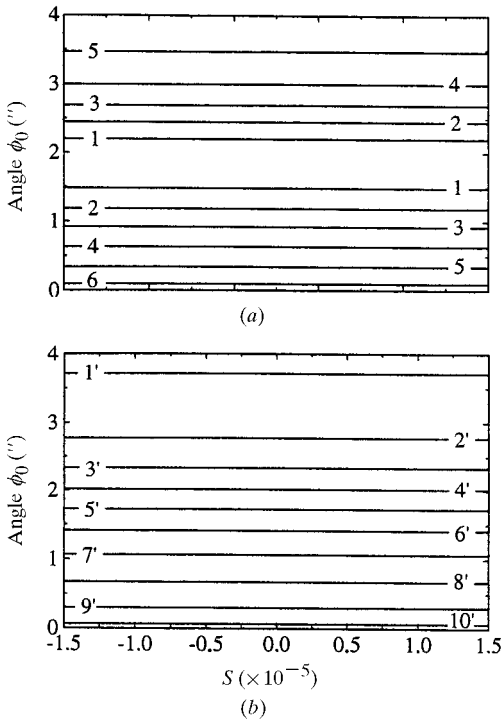


Fig. 5. Two-wave diffraction: (a) reflection coefficient  $R_{440}(S, \phi_0)$  and (b) the phase  $\Delta_{\text{dir}}^s$ . Contours 1–6 (a) correspond to  $R_{440} = 0.12, 0.1, 0.08, 0.06, 0.04, 0.02$  and 1'–10' (b) correspond to  $\Delta_{\text{dir}}^s = -5\pi/6, -3\pi/4, -2\pi/3, -7\pi/12, -\pi/2, -5\pi/12, -\pi/3, -\pi/4, -\pi/6, -\pi/12$ .

## 5.3. Interference of waves

When investigating the interference of waves, one should take into account the difference in their initial phases. In view of expressions (11) and (17), the difference in initial phases will be given by

$$\begin{aligned}\Psi^s &= \Psi_{\text{um}}^s - \Psi_{\text{dir}}^s \\ &= \Delta_{\text{um}}^s - \Delta_{\text{dir}}^s + \Phi_K + \Phi_L - \Phi_H \\ &= \Delta_{\text{um}}^s - \Delta_{\text{dir}}^s + \bar{\Phi}_3.\end{aligned}\quad (19)$$

The last equality holds exactly for non-absorbing crystals.  $\Delta_{\text{um}}^s - \Delta_{\text{dir}}^s$  represents a 'diffraction' path difference and  $\bar{\Phi}_3$  a 'geometrical' path difference between an *Umweg*-excited and a directly excited wave. Expression (19) shows that the difference in the initial phases is directly related to the triplet phase invariant.

In its turn, the 'diffraction' path difference, according to (16) and (18), is given by

$$\Delta^s = \Delta_{\text{um}}^s - \Delta_{\text{dir}}^s = \Delta(\phi_K) + \Lambda_3^s, \quad (20)$$

where

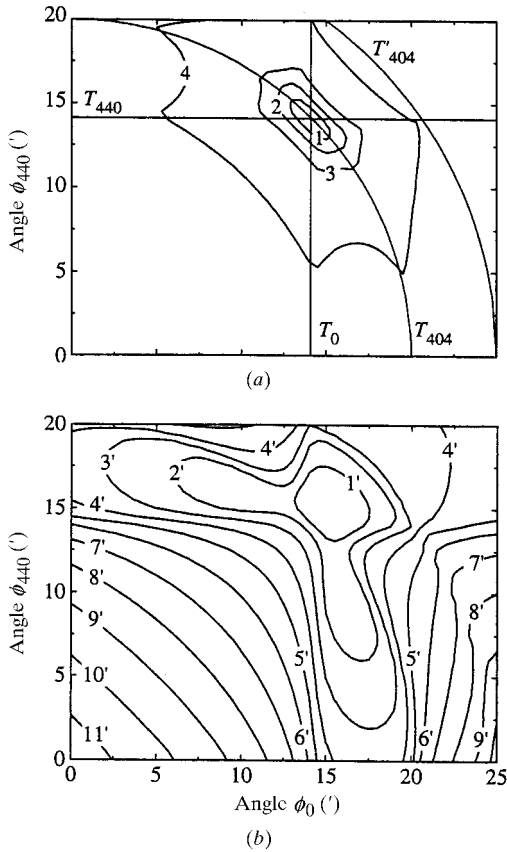


Fig. 6. Three-wave *Umweganregung* diffraction: (a) reflection coefficient  $R_{440}(\phi_0, \phi_{440})$  and (b) the phase  $\Delta_{\text{um}}^{\pi}$ . Contours 1-4 (a) correspond to  $R_{440} = 0.03, 0.02, 0.01, 0.001$  and 1'-11' (b) correspond to  $\Delta_{\text{um}}^{\pi} = -7\pi/6, -13\pi/12, -\pi, -11\pi/12, -5\pi/6, -3\pi/4, -2\pi/3, -7\pi/12, -\pi/2, -5\pi/12, -\pi/3$ .

$$\Lambda_3^s = \Lambda_K^s + \Lambda_L^s - \Lambda_H^s. \quad (21)$$

Hence, the change  $\Delta^s$  is caused solely by the  $K$  site moving out of the Ewald sphere. Figs. 8 and 9 give the distributions of  $\Delta^{\pi}$  in the coordinate systems  $O_{\phi_0\phi_{440}}$  and  $O_{S\phi_0}$ , respectively. The behaviour of  $\Delta^{\pi}$  is qualitatively rather well described by expression (20). As before, the approximation adopted in (20) fails along the lines  $T_0$ ,  $T_{440}$  and  $T_{404}$  in the vicinity of the Lorentz point. In addition, a shift of  $\Delta^{\pi}$  over the angle  $\Delta(\phi_K)$  is observed. As a result,  $\Delta^{\pi}$  will be given by  $-\pi/2$  for angles close to  $\phi_K = \phi_c$ . The above shift is due to the closeness of the sphere of radius  $(1 + \chi_0)^{1/2}/\lambda$  circumscribing the  $K$  site of the reciprocal lattice to the three-wave Lorentz point.

The above distributions of  $\Delta^{\pi}$  properly account for the phase dependence of the reflection coefficient distributions of a specularly diffracted wave. This can be demonstrated by examining the behaviour of the interference of the directly excited and the *Umweg*-excited waves, taking into account the distribution of  $\Delta^{\pi}$  and the value of the triplet phase invariant. For example, assume that the phase invariant  $\bar{\Phi}_3$  is zero. The regions of interference-induced amplification and attenuation of waves will then occur on the opposite sides of the  $T_{404}$  line. The amplification and attenuation will be observed as intensity variations of the directly excited wave, since

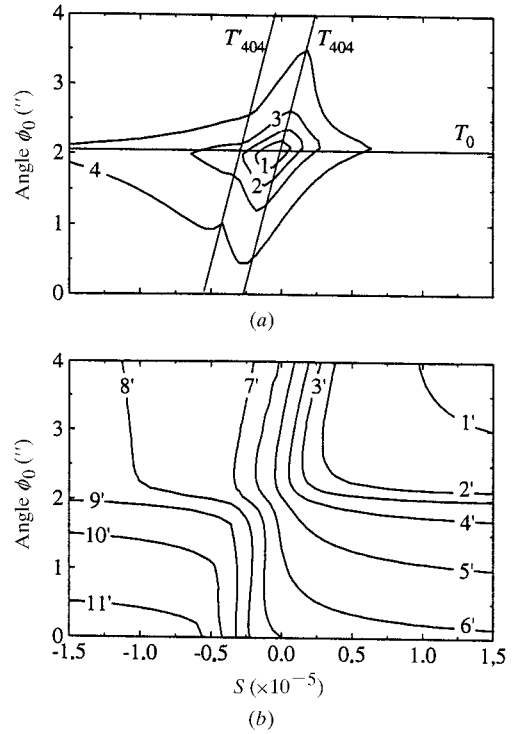


Fig. 7. Three-wave *Umweganregung* diffraction: (a) reflection coefficient  $R_{440}(S, \phi_0)$  and (b) the phase  $\Delta_{\text{um}}^{\pi}$ . Contours 1-4 (a) correspond to  $R_{440} = 0.035, 0.025, 0.015, 0.005$  and 1'-11' (b) correspond to  $\Delta_{\text{um}}^{\pi} = -11\pi/6, -5\pi/3, -3\pi/2, -4\pi/3, -7\pi/6, -\pi, -5\pi/6, -2\pi/3, -\pi/2, -\pi/3, -\pi/6$ .

this intensity is much higher than that of an *Umweg*-excited wave, as can be seen from Figs. 4(a) and 6(a) for the coordinate system  $O_{\phi_0\phi_{440}}$  and Figs. 5(a) and 7(a) for the coordinate system  $O_{S\phi_0}$ . Thus, for  $\phi_{404} > \phi_c$  under the coordinate system  $O_{\phi_0\phi_{440}}$  (see Fig. 1b) and for  $S > 0$  under the coordinate system  $O_{S\phi_0}$  (see Fig. 2b), attenuation will occur, while, for  $\phi_{404} < \phi_c$  and  $S < 0$ , amplification will be observed. A change in the value of the triplet phase invariant by  $\pi$  will reverse the order of appearance of the regions of amplification and attenuation (see Figs. 1d and 2d).

Now let the phase invariant be  $-\pi/2$ . The interference of two waves will then consist of their attenuation in the vicinity of line  $T_{404}$  (see Figs. 1a and 2a). For a triplet phase invariant  $\pi/2$ , the situation will be reversed, *i.e.* amplification of waves will be observed (see Figs. 1c and 2c). The distributions of the reflection coefficients of a specularly diffracted wave for intermediate values of the triplet phase invariant can be interpreted in a similar way.

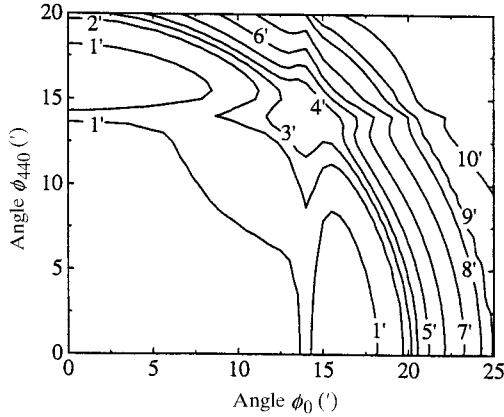


Fig. 8. The distribution of  $\Delta^\pi$  under the coordinate system  $O_{\phi_0\phi_{440}}$ . Level curves 1'–10' correspond to  $\Delta^\pi = -3\pi/4, -2\pi/3, -7\pi/12, -\pi/2, -5\pi/12, -\pi/3, -\pi/4, -\pi/6, -\pi/12, 0$ .

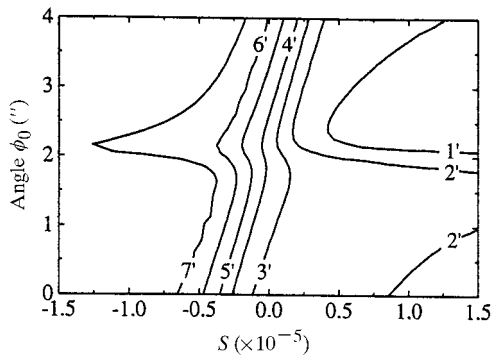


Fig. 9. The distribution of  $\Delta^\pi$  under the coordinate system  $O_{S\phi_0}$ . Contours 1'–7' correspond to  $\Delta^\pi = -\pi, -5\pi/6, -2\pi/3, -\pi/2, -\pi/3, -\pi/6, 0$ .

We note that, in the vicinity of the Lorentz point, some qualitative disagreement between the calculated reflection coefficients and those obtained using the above-simplified model is observed. This is because the present model does not take into account the actual energy transfer from wave  $H$  to wave  $K$ , resulting in a general decrease in the reflection coefficients in the vicinity of the Lorentz point.

#### 5.4. Polarization and phase sensitivity

The phase sensitivity of a specularly diffracted wave has so far been discussed for a  $\pi$ -polarized incident wave. The phase sensitivity for a  $\sigma$ -polarized incident wave will now be discussed.

Expression (16) for the diffraction geometry in question states that the phases  $\Delta_{\text{dir}}^s$  for  $\sigma$ - and  $\pi$ -polarized incident radiation in the two-wave case will differ by  $\pi$  because  $\Lambda_{440}^\sigma = 0$  and  $\Lambda_{440}^\pi = -\pi$ . On the other hand, (18) indicates that the distributions of phases  $\Delta_{\text{um}}^s$  of *Umweg*-excited waves for  $\sigma$ - and  $\pi$ -polarized incident radiation are similar because  $\Lambda_{044}^\sigma + \Lambda_{404}^\sigma = 0$  and  $\Lambda_{044}^\pi + \Lambda_{404}^\pi \equiv 0 \pmod{2\pi}$ . Eventually, the phases  $\Delta^\sigma$  and  $\Delta^\pi$  will differ by  $\pi$ , as given by (21). According to the present model, this will cause the regions of amplification and attenuation to appear in reverse order. Numerical calculations confirm the above conclusion. This is illustrated in Fig. 10 where the spectral and angular distribution of the reflection coefficient of a specularly diffracted wave is given for the  $\sigma$ -polarized radiation and  $\Phi_3 = 0$ . For comparison, see Fig. 2(b) for the  $\pi$ -polarized radiation.

As given by (20), the distributions of  $\Delta^s$  for the two polarization states are similar when  $\Lambda_3^\pi \equiv 0 \pmod{2\pi}$  ( $\Lambda_3^\sigma$  is always equal to zero), hence the regions of amplification and attenuation also coincide. Thus, the phase behaviour of the reflection coefficients of a specularly diffracted wave for the two polarization states will be similar under the condition that

$$\cos 2\theta_H \cos 2\theta_K \cos 2(\theta_H + \theta_K) > 0. \quad (22)$$

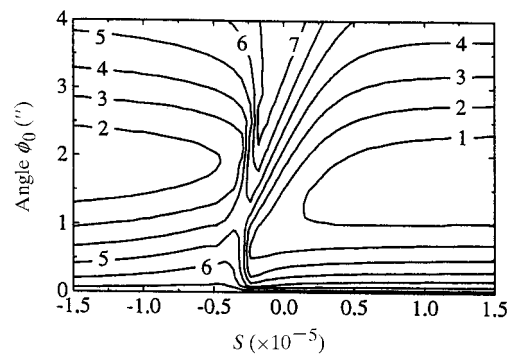


Fig. 10. Reflection coefficient  $R_{440}(S, \phi_0)$  for  $\sigma$ -polarized incident radiation and  $\Phi_3 = 0$ . Contours 1–7 correspond to  $R_{440} = 0.175, 0.15, 0.125, 0.1, 0.075, 0.05, 0.025$ .



This condition follows from (21) and (15) in view of  $2\theta_L \cong 2\pi - 2(\theta_H + \theta_K)$  for the diffraction geometry in question.

### 5.5. Diffraction geometry and phase sensitivity

As follows from expressions (19) and (20), for a fixed value of the triplet phase invariant, the order of appearance of the interference-induced amplification and attenuation regions for  $\sigma$ -polarized incident radiation is dependent on the position of the  $K$  site with respect to the Ewald sphere, rather than on the three-wave diffraction geometry, *i.e.* it is independent of the diffraction vectors  $\mathbf{H}$  and  $\mathbf{K}$  of a particular configuration. In particular, when the  $K$  site moves out of the Ewald sphere for  $\sigma$  polarization and  $\bar{\Phi}_3 = 0$ , the attenuation region will follow the amplification region.

On the other hand, during the spectral scanning of the three-wave region, the direction of movement of the  $K$  site with respect to the Ewald sphere will vary, depending on the particular configuration. Thus, as the incident wavelength increases (or the spectral parameter  $S$  decreases), the  $K$  site will move out of the Ewald sphere when

$$C = \mathbf{H} \cdot \mathbf{K} - \mathbf{K}^2 < 0, \quad (23)$$

*i.e.* when the angle included between vectors  $\mathbf{K}$  and  $\mathbf{L}$  is obtuse. Thus, for  $\sigma$  polarization and  $\bar{\Phi}_3 = 0$ , the attenuation region will follow the amplification region when  $S$  decreases, subject to condition (23) (see Fig. 10). Accordingly, the  $K$  site will move into the Ewald sphere on the condition that  $C > 0$ .

## 6. Conclusions

We have proposed a method for determining the value of the triplet phase invariant for thin crystal surface layers from diffracted intensity distributions and a model of analysing the phase sensitivity of the reflection coefficients of a specularly diffracted wave in the case of three-wave grazing-incidence X-ray diffraction. The latter is based on the interference of the directly excited and the *Umweg*-excited specularly diffracted waves. This model seems to account for the phase sensitivity properly, as well as the behaviour of an involved specularly diffracted wave as a function of the triplet phase invariant, the polarization state of the incident wave and the diffraction geometry. Very recently, we have carried out the proposed experiment and indeed observed the predicted phase effect on the reflection coefficients in

X-ray spectral scans using synchrotron radiation (Chang *et al.*, 1998).

## References

- Afanas'ev, A. M. & Melkonyan, M. K. (1983). *Acta Cryst.* **A39**, 207–210.
- Andreev, A. V. (1985). *Usp. Fiz. Nauk*, **145**, 113–137. (In Russian.)
- Andreev, A. V., Gorshkov, M. E. & Ilinskiy, Yu. A. (1985). *Dokl. Akad. Nauk SSSR*, **282**, 69–72. (In Russian.)
- Andreev, A. V., Kov'ev, E. K., Matveev, Yu. A. & Ponomarev, Yu. V. (1982). *JETP Lett.* **35**, 412–414. (In Russian.)
- Chang, S. L. (1982). *Phys. Rev. Lett.* **48**, 163–166.
- Chang, S. L., Huang, Y. S., Chao, C. H., Tang, M. T. & Stetsko, Yu. P. (1998). *Phys. Rev. Lett.* **80**, 301–304.
- Chang, S. L. & Tang, M. T. (1988). *Acta Cryst.* **A44**, 1065–1072.
- Chang, S. L. & Valladares, J. A. P. (1985). *Appl. Phys.* **A37**, 57–64.
- Chapman, L. D., Yoder, D. R. & Colella, R. (1981). *Phys. Rev. Lett.* **46**, 1578–1581.
- Collella, R. (1974). *Acta Cryst.* **A30**, 413–423.
- Cowan, P. L. (1985). *Phys. Rev. B*, **32**, 5437–5439.
- Hart, M. & Lang, A. R. (1961). *Phys. Rev. Lett.* **7**, 120–121.
- Høier, R. & Aanestad, A. (1981). *Acta Cryst.* **A37**, 787–794.
- Hümmer, K. & Billy, H. W. (1986). *Acta Cryst.* **A42**, 127–133.
- Hümmer, K., Weckert, E. & Bondza, H. (1989). *Acta Cryst.* **A45**, 182–187.
- Hung, H. H. & Chang, S. L. (1989). *Acta Cryst.* **A45**, 823–833.
- Hung, H. H. & Chang, S. L. (1993). *Europhys. Lett.* **23**, 415–420.
- Juretschke, H. J. (1982a). *Phys. Lett.* **A92**, 183–185.
- Juretschke, H. J. (1982b). *Phys. Rev. Lett.* **48**, 1487–1489.
- Juretschke, H. J. (1986). *Phys. Status Solidi B*, **135**, 455–466.
- Kambe, K. & Miyake, S. (1954). *Acta Cryst.* **7**, 218–219.
- Kshevetskiy, S. A., Stetsko, Yu. P. & Sheludko, S. A. (1987). *Kristallografiya*, **32**, 308–310. (In Russian.)
- Mo, F., Haubach, B. C. & Thorkildsen, G. (1988). *Acta Chem. Scand. Ser. A*, **42**, 130–138.
- Post, B. (1977). *Phys. Rev. Lett.* **39**, 760–763.
- Renninger, M. (1937). *Z. Phys.* **106**, 141–176.
- Sheludko, S. A. (1987). Doctoral thesis, Chernovtsy University, Ukraine. (In Russian.)
- Shen, Q. (1998). *Phys. Rev. Lett.* **80**, 3268–3271.
- Shen, Q. & Colella, R. (1988). *Acta Cryst.* **A44**, 17–21.
- Stepanov, S. A., Kondrashkina, E. A. & Novikov, D. V. (1991). *Nucl. Instrum. Methods*, **A301**, 350–357.
- Stetsko, Yu. P. (1990). Doctoral thesis, Chernovtsy University, Ukraine. (In Russian.)
- Stetsko, Yu. P. & Chang, S. L. (1997). *Acta Cryst.* **A53**, 28–34.
- Tseng, T. P. & Chang, S. L. (1990). *Acta Cryst.* **A46**, 567–576.
- Wagner, E. (1923). *Phys. Z.* **21**, 94–98.
- Weckert, E. & Hümmer, K. (1997). *Acta Cryst.* **A53**, 108–143.